Finite-temperature order-disorder phase transition in a frustrated bilayer quantum Heisenberg antiferromagnet in strong magnetic fields

Johannes Richter,[1] Oleg Derzhko,[1,2,3] and Taras Krokhmalskii[2]
[1]*Institut für Theoretische Physik, Universität Magdeburg, P.O. Box 4120, D-39016 Magdeburg, Germany*
[2]*Institute for Condensed Matter Physics, National Academy of Sciences of Ukraine, 1 Svientsitskii Street, L'viv-11, 79011, Ukraine*
[3]*National University "Lvivska Politechnika," 12 S. Bandera Street, L'viv, 79013, Ukraine*
(Received 30 June 2006; revised manuscript received 2 October 2006; published 27 October 2006)

We investigate the thermodynamic properties of the frustrated bilayer quantum Heisenberg antiferromagnet at low temperatures in the vicinity of the saturation magnetic field. The low-energy degrees of freedom of the spin model are mapped onto a hard-square gas on a square lattice. We use exact diagonalization data for finite spin systems to check the validity of such a description. Using a classical Monte Carlo method we give a quantitative description of the thermodynamics of the spin model at low temperatures around the saturation field. The main peculiarity of the considered two-dimensional Heisenberg antiferromagnet is related to a phase transition of the hard-square model on the square lattice, which belongs to the two-dimensional Ising model universality class. It manifests itself in a logarithmic (low-) temperature singularity of the specific heat of the spin system observed for magnetic fields just below the saturation field.

DOI: 10.1103/PhysRevB.74.144430 PACS number(s): 75.10.Jm, 75.45.+j

I. INTRODUCTION

The quantum Heisenberg antiferromagnet (HAFM) on geometrically frustrated lattices has attracted much attention during the last years.[1,2] Besides intriguing quantum ground-state phases at zero magnetic field those systems often show unconventional properties in finite magnetic fields such as plateaus and jumps in the magnetization curve, see, e.g., Ref. 3. The recent finding that a wide class of geometrically frustrated quantum spin antiferromagnets (including the kagomé, checkerboard, and pyrochlore lattices) has quite simple ground states in the vicinity of the saturation field,[4] namely independent localized-magnon states, has further stimulated studies of the corresponding frustrated quantum antiferromagnets at high magnetic fields.[5–9] In particular, the low-temperature high-field thermodynamics of various one- and two-dimensional frustrated quantum antiferromagnets which support localized-magnon states, can be discussed from a quite universal point of view by mapping the low-energy degrees of freedom of the quantum HAFM onto lattice gases of hard-core objects.[6–10] For instance, the kagomé (checkerboard) HAFM in the vicinity of the saturation field can be mapped onto a gas of hard hexagons (squares) on a triangular (square) lattice.[7–10] The exactly soluble hard-hexagon model exhibits an order-disorder second-order phase transition.[11] The hard-core lattice-gas model corresponding to the checkerboard HAFM consists of large hard squares on the square lattice with edge vectors $\vec{a}_1=(2,0)$ and $\vec{a}_2=(0,2)$ (i.e., there is a nearest-neighbor and next-nearest-neighbor exclusion). For the latter model no exact solution is available, but most likely there is also an order-disorder phase transition.[12] The existence of a phase transition in the hard-hexagon (large-hard-square) model would imply a corresponding finite-temperature transition of the corresponding spin model near saturation provided the low-temperature physics is correctly described by the hard-core lattice-gas model. However, at the present state of the investigations no conclusive statements for the kagomé and checkerboard antiferromagnets are available, since both models admit additional degenerate eigenstates not described by the hard-hexagon/large-hard-square model.[13,14] Furthermore, for these spin models precise statements on the gap between the localized-magnon ground states and the excitations are not available. Therefore the effect of additional ground states and the excited states on the low-temperature thermodynamics remains unclear.

The motivation for the present paper is to find and discuss another two-dimensional frustrated quantum HAFM, for which a hard-core lattice gas completely covers all low-energy states of the spin model in the vicinity of the saturation field and where all excitations are separated by a finite energy gap. For such a spin model one can expect that an order-disorder phase transition inherent in the hard-core lattice-gas model can be observed as a finite-temperature phase transition in the spin model. It might be worth noting that such a phase transition of course does not contradict the Mermin-Wagner theorem[15] that forbids magnetic long-range order (breaking the rotational symmetry) for the two-dimensional Heisenberg model at any nonzero temperature and at zero field.

A spin model which satisfies these requirements is a frustrated bilayer quantum HAFM. The investigation of the bilayer quantum HAFM was initially motivated by bilayer high-T_c superconductors[16] and has been continued until the present time, see, e.g., Ref. 17 and references therein. Below we will illustrate that the corresponding hard-core lattice-gas model is a model of hard squares on a square lattice, however, in difference to the checkerboard lattice with smaller hard squares with edge vectors $\vec{a}_1=(1,1)$ and $\vec{a}_2=(-1,1)$ (i.e., there is a nearest-neighbor exclusion, only, cf. Fig. 1). This hard-square model exhibits an order-disorder phase transition.[11,18,19] In the context of different universality classes discussed in Ref. 9 the frustrated bilayer quantum HAFM is the first example of a spin system which belongs to the universality class of (small) hard squares.

The paper is organized as follows. First, we specify the frustrated bilayer model and illustrate the corresponding

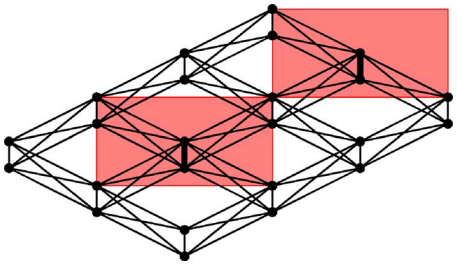

FIG. 1. (Color online) The frustrated bilayer antiferromagnet (black lines). The vertical bonds have the strength J_2 whereas all other bonds have the strength J_1. The trapping cells (vertical bonds) occupied by localized magnons are shown by fat lines. The auxiliary square lattice is a simple square lattice filled by hard squares (indicated as red squares) which correspond to localized magnons.

localized-magnon states (Sec. II). Then in Sec. III we calculate the contribution of the independent localized-magnon states to the thermodynamic quantities using the hard-square model. We compare our results with exact diagonalization data for finite spin-1/2 Heisenberg systems of up to $N=32$ sites. Finally, in Sec. IV we report the low-temperature high-field thermodynamic quantities obtained on the basis of Monte Carlo simulations for hard squares focusing on the (low-) temperature dependence of the specific heat in the vicinity of the saturation field.

II. THE FRUSTRATED BILAYER ANTIFERROMAGNET AND INDEPENDENT LOCALIZED MAGNONS

To be specific, we consider the nearest-neighbor Heisenberg antiferromagnet in an external magnetic field on the lattice shown in Fig. 1. This lattice may be viewed as a two-dimensional version of the frustrated two-leg ladder considered in Refs. 20–22 (for some similar models see Ref. 23). The Heisenberg Hamiltonian of N quantum spins of length s reads

$$H = \sum_{(nm)} J_{nm}\left(\frac{1}{2}(s_n^+ s_m^- + s_n^- s_m^+) + \Delta s_n^z s_m^z\right) - hS^z. \qquad (1)$$

Here the sum runs over the bonds (edges) which connect the neighboring sites (vertices) on the spin lattice shown in Fig. 1. $J_{nm}>0$ are the antiferromagnetic exchange constants between the sites n and m which take two values, namely, J_2 for the vertical bonds and J_1 for all other bonds. $\Delta \geqslant 0$ is the exchange interaction anisotropy parameter, h is the external magnetic field, and $S^z=\Sigma_n s_n^z$ is the z-component of the total spin. In our exact diagonalization studies reported below we will focus on $s=1/2$ and $\Delta=1$.

We note that the Hamiltonian (1) commutes with the operator S^z and hence we may consider the subspaces of its eigenstates with different values of S^z separately. Evidently, the fully polarized state $|0\rangle=|s,\ldots,s\rangle$ is the eigenstate of the Hamiltonian (1) with $S^z=Ns$ and can be considered as the vacuum state with respect to the number of excited magnons. This state is the ground state for high magnetic fields.

Consider next the one-magnon subspace with $S^z=Ns-1$. The one-particle energy is given by $\Lambda_{\mathbf{k}}^{(1)}=-s[J_2+\Delta(8J_1+J_2)]+h$ and $\Lambda_{\mathbf{k}}^{(2)}=s[4J_1(\cos k_x+\cos k_y)+J_2-\Delta(8J_1+J_2)]+h$ (here $k_\alpha=2\pi n_\alpha/M_\alpha$, $n_\alpha=1,2,\ldots,M_\alpha$, $\alpha=x,y$, $M_xM_y=N/2$). Obviously, the excitation branch $\Lambda_{\mathbf{k}}^{(1)}$ is dispersionless and it becomes the lower one when $J_2>4J_1$. Throughout this paper we assume $J_2 \geqslant 4J_1$. Then the saturation field is given by $h_1=s[J_2+\Delta(8J_1+J_2)]$.

The $N/2$ dispersionless one-magnon excitations can be written as localized excitations on the $N/2$ vertical bonds, i.e., $|1\rangle=|\mathrm{lm}\rangle_v|s,\ldots,s\rangle_e$ is an eigenstate of Eq. (1) in the subspace with $S^z=Ns-1$ with the zero-field eigenvalue $E_{\mathrm{FM}}-\epsilon_1$, where $E_{\mathrm{FM}}=4N\Delta s^2J_1+N\Delta s^2J_2/2$ and $\epsilon_1=s[J_2+\Delta(8J_1+J_2)]$. In $|1\rangle$ the first part is the localized one-magnon excitation on the vertical bond number v, i.e., $|\mathrm{lm}\rangle_v=2^{-1/2}(|s,s-1\rangle-|s-1,s\rangle)_v$ and the second part $|s,\ldots,s\rangle_e$ is the fully polarized environment.

We pass to the subspaces with $S^z=Ns-2,Ns-3,\ldots,Ns-n_{\max}$, where $n_{\max}=N/4$. We can easily construct many-particle states in these subspaces using the localized-magnon states. Explicitly the wave function of n independent localized magnons has the form

$$|n\rangle = |\mathrm{lm}\rangle_{v_1}\cdots|\mathrm{lm}\rangle_{v_i}\cdots|\mathrm{lm}\rangle_{v_n}|s,\ldots,s\rangle_e. \qquad (2)$$

It is important to note that any two vertical bonds v_i and v_j in Eq. (2) where localized magnons live are not allowed to be direct neighbors. The energy of the n independent localized-magnon state (2) in zero field $h=0$ is $E_n=E_{\mathrm{FM}}-n\epsilon_1$. Since n independent localized magnons can be put on the bilayer in many ways, the eigenstates (2) are highly degenerate. We denote this degeneracy by $g_N(n)$, that is the number of ways to put n hard squares on a lattice of $\mathcal{N}=N/2$ sites (see Fig. 1). According to Refs. 4 and 24 the independent localized-magnon states (2) are the states with the lowest energy in the corresponding subspaces. Moreover, they are linearly independent (orthogonal type in the nomenclature of Ref. 14) and form an orthogonal basis in each subspace.[14] Due to their linear independence they all contribute to the partition function of the spin system.

In the presence of an external field the eigenstates (2) have the energy $E_n(h)=E_{\mathrm{FM}}-hsN-n(\epsilon_1-h)$. At the saturation field, $h=h_1=\epsilon_1$, they all are ground states and the ground-state energy $E_n(h_1)$ does not depend on n. As a result the ground-state magnetization curve exhibits a jump at the saturation field. This jump is accompanied by a preceding wide plateau, where the width of this plateau can be obtained following the arguments given in Ref. 22 and from finite-size data. We find for $s=1/2$, $\Delta=1$ a plateau width of $h_1-h_2=4J_1$. This plateau belongs to the twofold degenerate ground state with maximum density $n_{\max}=N/4$ of localized magnons, the so-called magnon crystal,[4] where all localized magnons occupy only one of the two sublattices of the underlying square lattice.

Furthermore, the degeneracy of independent localized-magnon states at the saturation field $\mathcal{W}=\Sigma_{n=0}^{n_{\max}}g_N(n)$ grows exponentially with the system size N that implies a nonzero ground-state residual entropy $\mathcal{S}=k\lim_{N\to\infty}(\ln \mathcal{W}/N)=0.2037\ldots k$ (see Ref. 19 and also below). Due to their high degeneracy the independent localized-magnon states are also

dominating the thermodynamic properties at low temperatures for magnetic fields around the saturation field as we will discuss in detail below.

III. HARD-SQUARE MODEL

We want to calculate the contribution of the independent localized magnons to the canonical partition function of the spin system,

$$Z_{\rm lm}(T,h,N) = \sum_{n=0}^{n_{\rm max}} g_N(n)\exp\left(-\frac{E_n(h)}{kT}\right)$$
$$= \exp\left(-\frac{E_{\rm FM}-hsN}{kT}\right)\sum_{n=0}^{n_{\rm max}} g_N(n)\exp\left(\frac{\mu}{kT}n\right), \quad (3)$$

where $\mu=\epsilon_1-h=h_1-h$. It is apparent that $g_N(n)$ is the canonical partition function $Z(n,\mathcal{N})$ of n hard squares on a square lattice of $\mathcal{N}=N/2$ sites, whereas $\Xi(T,\mu,\mathcal{N})=\Sigma_{n=0}^{n_{\rm max}} g_N(n)\exp(\mu n/kT)$ is the grand canonical partition function of hard squares on a square lattice of $\mathcal{N}=N/2$ sites and μ is the chemical potential of the hard squares. As a result we arrive at the basic relation between the localized-magnon contribution to the canonical partition function of the spin model and the grand canonical partition function of the hard-square model,

$$Z_{\rm lm}(T,h,N) = \exp\left(-\frac{E_{\rm FM}-hsN}{kT}\right)\Xi(T,\mu,\mathcal{N}). \quad (4)$$

Equation (4) yields the Helmholtz free energy of the spin system $F_{\rm lm}(T,h,N)=-kT\ln Z_{\rm lm}(T,h,N)$, whereas the entropy S, the specific heat C, and the magnetization $M=\langle S^z\rangle$ are given by the usual formulas, $S_{\rm lm}(T,h,N)=-\partial F_{\rm lm}(T,h,N)/\partial T$, $C_{\rm lm}(T,h,N)=T\partial S_{\rm lm}(T,h,N)/\partial T$, and $M_{\rm lm}(T,h,N)=sN-kT\partial\ln\Xi(T,\mu,\mathcal{N})/\partial\mu$.

We use exact diagonalization data to check this picture for the $s=1/2$ isotropic Heisenberg system (1) of $N=16$ and $N=20$ sites (full diagonalization) and $N=32$ (only in the subspaces with $S^z=16,\ldots,11$) imposing periodic boundary conditions. We fix the energy scale by putting $J_1=1$. For the vertical exchange bonds we consider $J_2=4$, 5, and 10.

First we compare the degeneracies $g_N(n)$ of the localized n-magnon states calculated for spin systems of sizes $N=16$, 20, and 32 with the corresponding values $Z(n,N/2)$ of the hard-square model. As expected we find complete agreement between both models for $J_2>4J_1$. As an example we give here the numbers for $N=20$: $g_{20}(n)=1$, 10, 25, 20, 10, and 2 for $n=0$, 1, 2, 3, 4, and 5. For $J_2=4J_1$ the spin system has one extra state for $n=1$, i.e., in the one-magnon sector, since the dispersive mode $\Lambda_{\mathbf{k}}^{(2)}$ and the dispersionless mode $\Lambda_{\mathbf{k}}^{(1)}$ are degenerate at $\mathbf{k}=(\pi,\pi)$.

To estimate the relevance of excited states, not described by the localized-magnon scenario, we have determined the thermodynamically relevant energy separation $\Delta_{\rm DOS}$ between the localized-magnon states and the other states of the spin system by calculating the integrated low-energy density of states at saturation field. We define $\Delta_{\rm DOS}$ as that energy value above the localized-magnon ground-state energy, where the contribution of the higher-energy states to the integrated density of states becomes as large as the contribution of the localized-magnon states. For both values $J_2=5$ and 10 we find $\Delta_{\rm DOS}\approx 1$ independent of the size of the system N. We can expect that the contribution of the localized-magnon states to the partition function is dominating for temperatures kT significantly smaller than $\Delta_{\rm DOS}$.

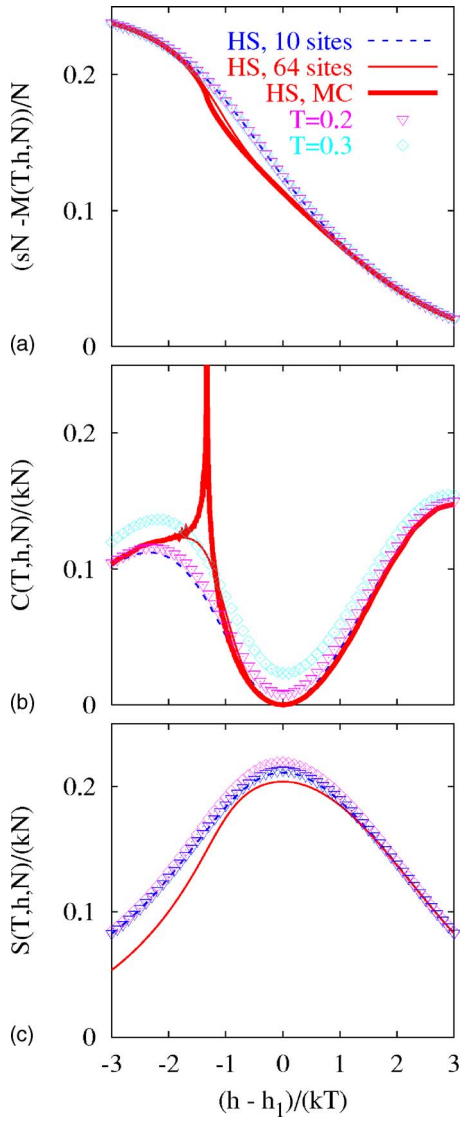

FIG. 2. (Color online) The magnetization $[sN-M(T,h,N)]/N$ (a), the specific heat $C(T,h,N)/kN$ (b), and the entropy $S(T,h,N)/kN$ (c) as functions of $(h-h_1)/kT$. Symbols correspond to the exact diagonalization data [$N=20$, $J_2=5$, $kT=0.2$ (triangles), and $kT=0.3$ (diamonds)]. Thin lines correspond to the results for a small hard-square system $\mathcal{N}=10$ (thin dotted lines) and $\mathcal{N}=64$ (thin solid lines). The exact diagonalization data for the temperatures up to $kT=0.1$ coincide with the corresponding data for the $\mathcal{N}=10$ hard-square system. We also show by thick lines the Monte Carlo simulation results for the magnetization and the specific heat for a hard-square system of sizes up to 800×800 sites.

In Fig. 2 we present our results for the magnetization, the specific heat, and the entropy (panels from top to bottom) for

the spin system of size $N=20$ (triangles and diamonds). We compare those data with the corresponding data taking into account only the contribution of independent localized-magnon states, described by the finite hard-square model of $\mathcal{N}=10$ sites (thin dotted lines). Up to $kT\approx 0.1$ both data sets coincide, demonstrating that the hard-square description perfectly works at low temperatures. But we observe good agreement also for higher temperatures up to $kT\approx 0.3$, indicating that the independent localized magnons still dominate the thermodynamic quantities. Further increasing kT, the high-energy states more and more contribute to the partition function and the hard-square description loses its validity. Note that an identical statement can be made for $N=16$ ($\mathcal{N}=8$).

IV. LOW-TEMPERATURE THERMODYNAMICS AROUND THE SATURATION FIELD

Now we discuss the low-temperature high-field thermodynamics of the frustrated bilayer quantum HAFM using the results for the hard-square model. From Fig. 2(b) it is obvious that fixing the temperature to a sufficiently low value the spin system can be driven through a phase transition by increasing the magnetic field h towards the saturation field h_1. On the other hand, we can fix the magnetic field slightly below the saturation field and vary the temperature. Then the phase transition is driven by the temperature and the specific heat exhibits a singularity at a critical temperature $T_c(h)$, see Fig. 3, where we show the results of a Monte Carlo simulation for large hard-square systems (periodic cells with up to 800×800 sites and 3×10^6 steps) for the specific heat for two values of the magnetic field. The data clearly indicate a phase transition which occurs in the hard-square model at $z_c=3.7962\ldots$, i.e., at $[(h_1-h)/kT]_c=\ln z_c\approx 1.3340$ which yields $kT_c(h)\approx(h_1-h)/1.3340$. The corresponding order parameter is the difference of the density (of hard squares or localized magnons in hard-square or spin language, respectively) on the A- and B-sublattices of the underlying square lattice.[11] For $[(h_1-h)/kT]_c<\ln z_c$ [i.e., for $T>T_c(h)$, $h<h_1$] both sublattices are equally occupied, but for $[(h_1-h)/kT]_c>\ln z_c$ [i.e., for $T<T_c(h)$, $h<h_1$] one of two sublattices is more occupied than the other. Therefore in the ordered phase the translational symmetry of the spin (hard-square) system is broken. Finally, at $T=0$ only one sublattice is occupied and the other is empty and the ground state of the spin system is a magnon-crystal state, see Sec. II.

We can estimate the critical temperature for a fixed deviation of the field from the saturation value using the above given expression for $kT_c(h)$. For $1-h/h_1=0.02$ we find $kT_c/h_1\approx 0.0150$, whereas for $1-h/h_1=0.01$ we have $kT_c/h_1\approx 0.0075$ and for the spin system with $J_2=5$ we find for $h=8.91J_1$ ($h=8.82J_1$) $kT_c\approx 0.0675J_1$ ($kT_c\approx 0.1349J_1$). Such temperatures are within a temperature range where the hard-square description for finite systems works *perfectly* well (see Figs. 2 and 3). However, one may expect that the scenario of the phase transition may hold also at temperatures, for which the localized-magnon states are still dominant but also higher-energy states of the spin system not described by the hard-square model contribute to the partition function.

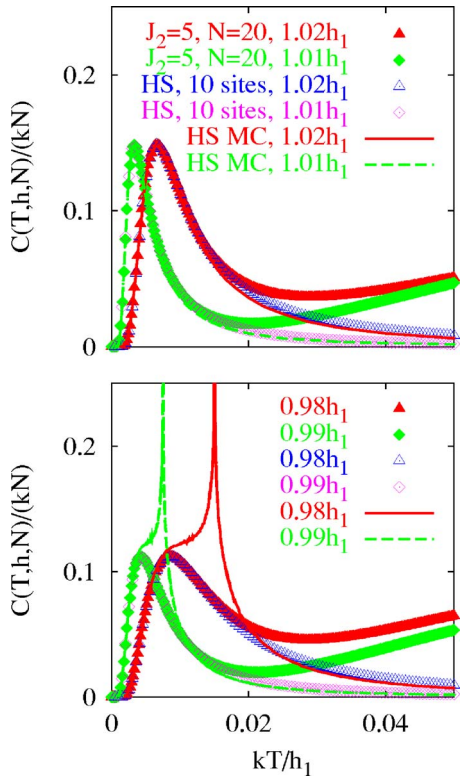

FIG. 3. (Color online) The temperature dependence of the specific heat $C(T,h,N)/kN$ for $h=1.01h_1$ (broken lines, diamonds) and $h=1.02h_1$ (solid lines, triangles) (upper panel) and for $h=0.99h_1$ (broken lines, diamonds) and $h=0.98h_1$ (solid lines, triangles) (lower panel). The results of Monte Carlo simulations for a hard-square system of sizes up to 800×800 sites are shown by lines. We also report the corresponding results for the hard-square system with $\mathcal{N}=10$ (open symbols) and the exact diagonalization data for the finite spin system with $N=20$, $J_2=5$ (closed symbols).

We mention that the hard-square model belongs to the two-dimensional Ising model universality class[11,25,26] with the critical exponents $\beta=1/8$ for the order parameter and $\alpha=0$ for the specific heat, i.e., the specific heat shows a logarithmic singularity at the critical point. Note that this universality class is different from the one of the hard-hexagon model.[11] Thus the low-temperature peak (singularity) in the temperature dependence of the specific heat in the vicinity of the saturation field is a spectacular sign of highly degenerate independent localized-magnon states of the frustrated bilayer quantum HAFM. Their ordering leads to the hard-square type peculiarity just below the saturation field.

Another thermodynamic quantity of interest is the curve of constant entropy as a function of magnetic field and temperature. Since hard-square description implies the dependence of the entropy only on $(h_1-h)/kT$ this curve is similar to an ideal paramagnet. Therefore the considered spin system is expected to exhibit a large magnetocaloric effect in the vicinity of the saturation field.[6,7,9]

Finally we note that the effect of the localized magnons is a pure quantum effect which disappears as s increasingly approaches the classical limit $s\to\infty$.[4]

From the experimental point of view it might be desirable to go away from the assumed "perfect" condition when in-plane bonds and interplane bonds (except the vertical bonds J_2) have the same strength J_1. For slightly different in-layer and interlayer J_1 interactions the flat excitation branch becomes weakly dispersive and the mapping of the low-energy degrees of freedom of the spin model onto the hard-square model becomes approximative. An interesting problem is to study the low-temperature strong-field properties of the spin model in this case. This problem is out of the scope of the present paper and we have left it for future studies. However, we may expect (see Ref. 8) that the main features of "the ideal model" survive for small deviations from the adopted relation for the bond strengths.

ACKNOWLEDGMENTS

The numerical calculations were performed using J. Schulenburg's *spinpack*. The present study was supported by the DFG (Projects No. 436 UKR 17/13/05 and Ri615/12-1). O.D. acknowledges the kind hospitality of the Magdeburg University in the summer of 2006.

[1] *Quantum Magnetism*, edited by U. Schollwöck, J. Richter, D. J. J. Farnell, and R. F. Bishop, Lecture Notes in Physics, Vol. 645 (Springer, Berlin, 2004).
[2] *Frustrated Spin Systems*, edited by H. T. Diep (World Scientific, Singapore, 2005).
[3] A. Honecker, J. Schulenburg, and J. Richter, J. Phys.: Condens. Matter **16**, S749 (2004).
[4] J. Schnack, H.-J. Schmidt, J. Richter, and J. Schulenburg, Eur. Phys. J. B **24**, 475 (2001); J. Schulenburg, A. Honecker, J. Schnack, J. Richter, and H.-J. Schmidt, Phys. Rev. Lett. **88**, 167207 (2002); J. Richter, J. Schulenburg, A. Honecker, J. Schnack, and H.-J. Schmidt, J. Phys.: Condens. Matter **16**, S779 (2004).
[5] J. Richter, O. Derzhko, and J. Schulenburg, Phys. Rev. Lett. **93**, 107206 (2004); O. Derzhko and J. Richter, Phys. Rev. B **72**, 094437 (2005).
[6] M. Zhitomirsky and A. Honecker, J. Stat. Mech.: Theory Exp. 2004, P07012.
[7] M. E. Zhitomirsky and H. Tsunetsugu, Phys. Rev. B **70**, 100403(R) (2004); M. E. Zhitomirsky and H. Tsunetsugu, Prog. Theor. Phys. Suppl. **160**, 361 (2005).
[8] O. Derzhko and J. Richter, Phys. Rev. B **70**, 104415 (2004).
[9] O. Derzhko and J. Richter, Eur. Phys. J. B **52**, 23 (2006).
[10] M. E. Zhitomirsky and H. Tsunetsugu (unpublished).
[11] R. J. Baxter, *Exactly Solved Models in Statistical Mechanics* (Academic Press, London, 1982).
[12] F. H. Ree and D. A. Chesnut, Phys. Rev. Lett. **18**, 5 (1967); A. Bellemans and R. K. Nigam, J. Chem. Phys. **46**, 2922 (1967); L. Lafuente and J. A. Cuesta, *ibid.* **119**, 10832 (2003).
[13] A. Honecker (private communication).
[14] H.-J. Schmidt, J. Richter, and R. Moessner, J. Phys. A **39**, 10673 (2006).
[15] N. D. Mermin and H. Wagner, Phys. Rev. Lett. **17**, 1133 (1966); **17**, 1307 (1966).
[16] A. W. Sandvik and D. J. Scalapino, Phys. Rev. Lett. **72**, 2777 (1994).
[17] G. S. Uhrig, K. P. Schmidt, and M. Grüninger, J. Phys. Soc. Jpn. **74**, 86 (2005); Ling Wang, K. S. D. Beach, and A. W. Sandvik, Phys. Rev. B **73**, 014431 (2006).
[18] R. J. Baxter, I. G. Enting, and S. K. Tsang, J. Stat. Phys. **22**, 465 (1980).
[19] R. J. Baxter, Ann. Comb. **3**, 191 (1999).
[20] M. P. Gelfand, Phys. Rev. B **43**, 8644 (1991).
[21] F. Mila, Eur. Phys. J. B **6**, 201 (1998).
[22] A. Honecker, F. Mila, and M. Troyer, Eur. Phys. J. B **15**, 227 (2000).
[23] I. Bose and S. Gayen, Phys. Rev. B **48**, 10653 (1993); E. Müller-Hartmann, R. R. P. Singh, C. Knetter, and G. S. Uhrig, Phys. Rev. Lett. **84**, 1808 (2000); B. Sutherland, Phys. Rev. B **62**, 11499 (2000); S. Chen and H. Büttner, Eur. Phys. J. B **29**, 15 (2002); V. R. Chandra and N. Surendran, Phys. Rev. B **74**, 024421 (2006).
[24] H.-J. Schmidt, J. Phys. A **35**, 6545 (2002).
[25] Z. Rácz, Phys. Rev. B **21**, 4012 (1980).
[26] W. Guo and H. W. J. Blöte, Phys. Rev. E **66**, 046140 (2002).